Pergamon

Int. J. Heat Mass Transfer. Vol. 38, No. 17, pp. 3231–3240, 1995

0017-9310/95 $9.50+0.00

0017-9310(95)00052-6

The generalized lagging response in small-scale and high-rate heating

DA YU TZOU

Department of Mechanical Engineering, The University of New Mexico, Albuquerque, NM 87131, U.S.A.

(*Received* 26 *April* 1994 *and in final form* 19 *January* 1995)

Abstract—The generalized lagging behavior in solids under high-rate heating is derived by precise correlation with the hyperbolic two-step model. The ballistic behavior of heat transport in the electron gas is found to be captured by the second-order effect of the phase lag of the heat flux vector. In contrast to the parabolic two-step model, the ballistic behavior results in a sharp wavefront in the history of heat propagation. The analytical expression for the thermal wave speed is derived. In comparison with the classical diffusion and the wave models, the two phase lags in the lagging response result in a much deeper thermal penetration depth and much higher temperature in the heat-affected zone.

INTRODUCTION

Research of high-rate heating on thin film structures has rapidly grown in recent years because of the advancement of short-pulse laser technologies and their applications to modern microfabrication technologies [1–5]. To date, the laser pulse can be shortened to the range of femtoseconds (10^{-15} s) [6–9], making controls of the penetration depth and the processing time of the material more effective and accurate. Complexity of this type of problem lies in (i) the *non-equilibrium* thermodynamic transition associated with shortening of the response time; (ii) the activation of *microstructural* effects due to the small penetration depth of the heat-affected zone or the thinness of the thin-film structures. For most engineering materials, these two factors merge. When the response time in metal films reduces to the range of picoseconds, it becomes comparable to the thermalization time (the time needed for the electron gas and the metal lattice to achieve thermodynamic equilibrium) and the relaxation time (the characteristic time for the activation of the ballistic behavior in the electron gas) in the phonon–electron system [10, 11]. The effect of phonon–electron interactions in this time-frame, therefore, needs to be incorporated in the heat transfer model and the formulation becomes microscopic in nature. Heat transport in dielectric crystals is another example [12]. If the response time is of the same order of magnitude as the relaxation time of the Umklapp process (the characteristic time in which momentum is non-conserving in phonon collisions, 10^{-10} to 10^{-12} seconds), the microscopic process describing the phonon scattering from grain boundaries needs to be accommodated. The microscopic effect, therefore, occurs in companion with the fast-transient process in heat transport. Owing to the complexity of the space–time interactions, the ASME Heat Transfer Division has organized two national conferences [13, 14] to identify the physical mechanisms governing the small-scale heat transfer in the fast-transient. The recent work by Tien and Chen [15], in addition, categorizes the regime maps in conductive and radiative heat transfer by various length-scales on the microscopic level.

The wave theory in heat conduction addresses the inertial effect in the short-time transient via a macroscopic approach. The discontinuity existing at the thermal wavefront results in several unique features, including the thermal shock formation [16–19] and the thermal resonance phenomenon [20, 21], which cannot be depicted by diffusion. The review articles [22–25] have summarized about three hundred papers for an overview of past research developed in this direction. Despite the Cattaneo–Vernotte equation [26–28] in the thermal wave theory being admissible within the framework of the extended irreversible thermodynamics [29], it assumes a macroscopic behavior averaged over many grains. When the microstructural effect becomes pronounced, as associated with shortening of the response time, the concept of macroscopic average may lose its physical support and the applicability of the thermal wave model becomes open to debate.

From a microscopic point of view, on the other hand, the energy exchange between electrons and phonons was described by Kaganov *et al* [30]. The resulting phenomenological two-step model [31] describing the temperatures of the electron gas and the metal lattice during short-pulse laser heating of metals has gained support from the recent advancement of short-pulse laser technologies [6–9, 32, 33]. By employing ultrafast lasers, the phonon–electron coupling factor in the two-step model has been successfully measured for several metals. The original

NOMENCLATURE

C_e, C_l volumetric heat capacity of the electron gas and the metal lattice [J m^{-3} K^{-1}]
C thermal wave speed [m s^{-1}]
G electron-phonon coupling factor [W m^{-3} K^{-1}]
h Planck constant [J s]
k Boltzmann constant [J K^{-1}]
K thermal conductivity [W m^{-1} K^{-1}]
n_a, n_e volumetric number density of atoms and free electrons, [m^{-3}]
N number of terms in the series truncation.
p Laplace transform parameter.
q heat flux [W m^{-2}]
R ratio of the two phase lags, τ_T/τ_q
S volumetric heat source [W m^{-3}]
t time [s]
T absolute temperature [K]
v_s speed of sound [m s^{-1}]
x space variable [μm].

Greek symbols
α thermal diffusivity [m^2 s^{-1}]
β dimensionless time
δ dimensionless space
θ dimensionless temperature
τ effective relaxation time based on the concept of effective conductivity [s]
τ_T, τ_q phase lags of the temperature gradient and the heat flux vector [s]
ω frequency in the Fourier transform domain.

Subscripts and superscripts
0 quantities calculated at 0 K
F quantities calculated at the Fermi surface.

expression of the phonon–electron coupling factor depends on the electron mean free time between collisions [30]. Later, by the use of Wiedemann–Franz's law, it was expressed in terms of the thermal conductivity [10]. It appears to the author that the two-step model formulated by Anisimov *et al.* [31] is essentially phenomenological and was not derived on a rigorous basis. It was not until Qiu and Tiens' recent work [11] that the phonon–electron coupling was *derived* from the solution of the Boltzmann equation in the absence of the electrical current during laser heating. In contrast to the classical approach [30, 31], the general derivation [11] reveals the *hyperbolic* nature of energy transport by electrons in metals. The relaxation time for heat transport in the electron gas is of the order of femtoseconds, which is about two orders of magnitude *smaller* than the phonon–electron thermalization time.

The present work emphasizes the fundamental structures of temperature *waves* depicted by the hyperbolic two-step model. A *single* energy equation governing the temperature of the metal lattice will be derived and attention focussed on the way in which the thermal disturbance propagates through it. Most importantly, for bringing together research efforts in macro- and micro-scale heat transfer, I shall continue the development of the dual-phase-lag model [34] and show that the second-order effect of the phase lag of the heat flux vector captures the ballistic behavior of heat transport in the electron gas.

THE HYPERBOLIC TWO-STEP MODEL

Qiu and Tien [11] derived the hyperbolic two-step radiation heating model based on the macroscopic averages of the electric and heat currents carried by electrons in the momentum space. In the absence of electric current during laser heating, they arrived at three coupled equations describing the one-dimensional energy exchange between phonons and electrons:

$$C_e\frac{\partial T_e}{\partial t} = -\frac{\partial q}{\partial x} - G(T_e - T_l) + S \tag{1a}$$

$$C_l\frac{\partial T_l}{\partial t} = G(T_e - T_l) \tag{1b}$$

$$\tau_F\frac{\partial q}{\partial t} + K\frac{\partial T_e}{\partial x} + q = 0. \tag{1c}$$

In equation (1c), the value of τ_F has been assumed small and the second-order terms and higher are neglected [11]. For metals, the externally supplied photons (the source term S) first increase the temperature of the electron gas as represented by equation (1a). Through the phonon–electron interactions, i.e. the second step, the hot electron gas heats up the metal lattice as represented by equation (1b). Equation (1c) describes the way in which heat propagates through the electron gas, i.e. the constitutive equation. The distinguishing feature between this and the Cattaneo–Vernotte equation for macroscopic thermal waves, however, is that energy transport depicted by equation (1) is for electrons on the microscopic scale and the thermal conductivity (K) in the phonon–electron system may depend on the temperature of the electron gas as well. The quantity τ_F is the relaxation time evaluated at the Fermi surface:

$$\tau_F = (2)^{4/3}\Lambda^{-1}\left(\frac{T_D}{T_l}\right)E_0E^{3/2} \tag{2}$$

where E_0 is the Fermi energy of electrons at 0 K, T_D

is the Debye temperature and Λ is a constant defined as

$$\Lambda = \frac{3\pi^2 P^2 (m/2)^{1/2}}{MkT_D}\left(\frac{3}{4\pi\Delta}\right)^{1/3} \quad (3)$$

with P standing for the transient matrix element, m the effective mass of electrons, M the atomic mass, T_D the Debye temperature, k the Boltzmann constant and Δ the averaged volume of the unit cell [11]. The energy exchange between phonons and electrons is characterized by the coupling factor G [10]:

$$G = \frac{\pi^4 (n_e v_s k)^2}{K}. \quad (4)$$

It depends on the number density of free electrons per unit volume n_e, the Boltzmann constant k and the speed of sound v_s:

$$v_s = \frac{k}{2\pi h}(6\pi^2 n_a)^{-1/3} T_D. \quad (5)$$

The phonon–electron coupling factor, through the speed of sound, further depends on the Planck constant (h), the atomic number density per unit volume (n_a) and the Debye temperature (T_D). The s-band approximation [10] provides an accurate estimate for the number density of free electrons in pure metals. The volumetric heat capacities of the electron gas and the metal lattice, C_e and C_l in equation 1(a) are, respectively, functions of the electron temperature (T_e) and the lattice temperature (T_l). Qiu and Tien [11] numerically solved equation (1) by considering a specific laser heating source ($S(x,t)$) with the laser wavelength in the visible light range. The film thickness is 0.1 μm and the laser-pulse duration is 96 fs. The predicted temperature change of the electron gas established in picoseconds agrees very well with the experimental data. The classical diffusion and the thermal wave models, because of the absence of modeling the microstructural effect in the short-time transient, predicted a *reversed* trend for the surface reflectivity at the rear surface of the thin film. The analysis supports the validity of the hyperbolic two-step model well when used for describing the heat transfer mechanisms during short-pulse laser heating of metals.

In exploring the *wave* structure of temperatures in equation (1), attention is focussed on the metal-lattice temperature, T_l, because it is a macroscopic quantity of major interest to practicing engineers. Since the temperature-dependent properties, such as the volumetric heat capacity of the electron gas, only affect the quantitative behavior of the temperature waves while the fundamental behavior remains the same, it will be assumed that all the thermal properties remain constant at this initial stage of exploration. Bearing this in mind, proceed to eliminate the electron temperature, T_e, from equation (1). I first differentiate equation (1a) with respect to t and equation (1c) with respect to x. I then combine equation (1a) with the results to eliminate the term of $\partial^2 q/\partial x\,\partial t$, rendering

$$K\frac{\partial^2 T_e}{\partial x^2} + \left(S + \tau_F \frac{\partial S}{\partial t}\right) = C_e \frac{\partial T_e}{\partial t} + C_e \tau_F \frac{\partial^2 T_e}{\partial t^2} + G(T_e - T_l) + \tau_F G \frac{\partial}{\partial t}(T_e - T_l). \quad (6)$$

The quantities T_e and $T_e - T_l$ in this equation can be related to the lattice temperature by equation (1b):

$$T_e = T_l + \frac{C_l}{G}\frac{\partial T_l}{\partial t}, \quad \text{consequently } T_e - T_l = \frac{C_l}{G}\frac{\partial T_l}{\partial t}. \quad (7)$$

Substituting equation (7) into (6), one obtains

$$\frac{\partial^2 T}{\partial x^2} + \left(\frac{C_l}{G}\right)\frac{\partial^3 T}{\partial x^2\,\partial t} + \frac{1}{K}\left(S + \tau_F \frac{\partial S}{\partial t}\right) = \tau_F\left(\frac{C_e C_l}{KG}\right)\frac{\partial^3 T}{\partial t^3} + \left(\frac{\tau_F (C_e + C_l)}{K} + \frac{C_e C_l}{KG}\right)\frac{\partial^2 T}{\partial t^2} + \left(\frac{C_e + C_l}{K}\right)\frac{\partial T}{\partial t} \quad (8)$$

where $T \equiv T_l$, the subscript 'l' in T_l has been neglected for the sake of convenience. In the case of $\tau_F = 0$, i.e. no ballistic behavior of heat transport in the electron gas, equation (8) reduces to the parabolic two-step equation [34]. The mixed-derivative term involving the second-order derivative in space and the first-order derivative in time, $(\partial^3 T/\partial x^2\,\partial t)$, is a special feature in both the parabolic and the hyperbolic two-step models. In the presence of τ_F, most importantly: (i) the time-derivative in the energy equation is raised to the *third order*; (ii) an *apparent* heat source term containing the time-derivative of the real heat source applied to the body, $(\partial S/\partial t)$, exists. While the third-order time-derivative intrinsically alters the fundamental structure of the temperature solution, the apparent heating in equation (8) resembles that in the classical thermal wave model [16–22, 35].

Along with the relaxation time of the electron gas (τ_F), the phonon–electron coupling factor G is the most important factor characterizing equation (8). In the case that τ_F approaches zero and G approaches infinity, implying that either the number density of free electrons (n_e) approaches infinity (refer to equation (4)) or the speed of sound approaches infinity (the atomic number density per unit volume n_a approaches zero according to equation (5)), equation (8) reduces to the classical diffusion equation. The Fourier law, leading to the diffusion equation, thus follows from these assumptions.

THE DUAL-PHASE-LAG CONCEPT

Equation (8) governing the lattice temperature brings in a new type of equation in conductive heat transfer. It includes both the microstructural effects (all the terms containing G) and the fast-transient response (all the terms containing τ_F). From a mathematical point of view, the third-order mixed-derivative term and the third-order time-derivative term dis-

tinguish equation (8) from the diffusion and the classical thermal wave equations.

Derivation of equation (1), and hence the combined equation (8), requires profound knowledge of quantum mechanics and the elastic and inelastic phonon–electron scattering processes in energy transport [10, 11]. The Boltzmann transport equation governing the distribution function of electrons and the redistribution of electrons among energy states during electron-lattice scattering, for example, may not be familiar to practicing engineers. In order to involve as many practicing engineers as possible in the rapid growth of microscale heat transfer, an equivalent formulation employing a *macroscopic* approach may be helpful. The macroscopic formulation is more familiar to practicing engineers, making it possible to extend their existing knowledge for the continuous development.

Including the phonon–electron interactions in metal films and pure phonon scattering in dielectric media, any physical process needs a *finite time* to take place. Like the previous study [34], these interactions on the *microscopic* level are viewed as retarding sources causing a *delayed* response on the *macroscopic* scale. Mathematically, this concept is illustrated by considering the following one-dimensional constitutive equation:

$$q(x, t+\tau_q) = -K\frac{\partial T(x, t+\tau_T)}{\partial x}. \tag{9}$$

This equation shows that the heat flux and the temperature gradient occur in a sequence of time. For $\tau_T > \tau_q$, heat first flows through a material volume located at x at time $t+\tau_q$. Microstructural interactions such as scattering of phonons by the lattice, the temperature gradient, as a result of heat flow at time $t+\tau_q$, establishes across the same material volume at a later time $t+\tau_T$. The physical time t is the instant at which physical observation on heat transport is made. Conservation of energy thus applies:

$$-\frac{\partial q(x, t)}{\partial x} + S(x, t) = C_p\frac{\partial T(x, t)}{\partial t}. \tag{10}$$

Equations (9) and (10) provides a set of *delayed* differential equations for determining the heat flux $q(x, t)$ and temperature $T(x, t)$. Just like the thermal conductivity and diffusivity, the two phase lags τ_T and τ_q are two additional *intrinsic thermal properties* of the medium. Aiming at an equivalent formulation to equation (8), assume small values of τ_T and τ_q so that (i) the second-order terms in τ_T and (ii) the third-order terms in τ_q and subsequent terms are negligible. The Taylor series expansion of equation (9) with respect to t then yields:

$$q(x, t)+\tau_q\frac{\partial q}{\partial t}(x, t)+\frac{\tau_q^2}{2}\frac{\partial^2 q}{\partial t^2}(x, t) \simeq -K\left(\frac{\partial T(x, t)}{\partial x}+\tau_T\frac{\partial^2 T(x, t)}{\partial x\,\partial t}\right). \tag{11}$$

Eliminating the heat flux q from equations (10) and (11) gives

$$\frac{\partial^2 T}{\partial x^2}+\tau_T\frac{\partial^3 T}{\partial x^2\,\partial t}+\frac{1}{K}\left(S+\tau_q\frac{\partial S}{\partial t}+\frac{\tau_q^2}{2}\frac{\partial^2 S}{\partial t^2}\right)=\frac{1}{\alpha}\frac{\partial T}{\partial t}+\frac{\tau_q}{\alpha}\frac{\partial^2 T}{\partial t^2}+\frac{\tau_q^2}{2\alpha}\frac{\partial^3 T}{\partial t^3}. \tag{12}$$

The second-order expansion of τ_q^2 induces an additional heat-source term, the second-order derivative in time, in the *apparent* heating. Because the heat source term does not affect the fundamental structure of the solution, the source terms in both equation (8) (the *microscopic* hyperbolic two-step model) and (12) (the *macroscopic* dual-phase-lag model) will be dropped when establishing their correlation. For $S = 0$, clearly, equation (8) and (12) are identical. Equating the corresponding coefficients, I have

$$\alpha = \frac{K}{C_e+C_l}, \quad \tau_T = \frac{C_l}{G} \tag{13a}$$

$$\frac{\tau_q}{\alpha} = \frac{\tau_F(C_e+C_l)}{K}+\frac{C_eC_l}{KG} \tag{13b}$$

$$\frac{\tau_q^2}{2\alpha} = \left(\frac{C_eC_l}{KG}\right)\tau_F. \tag{13c}$$

Equation (13a) expresses the *macroscopic* properties, α and τ_T, in the dual-phase-lag model in terms of the *microscopic* properties, G, C_e and C_l in the hyperbolic two-step model. Equations (13b) and (13c) seem to over-determine the remaining property τ_q, but they are essentially *the same* within the context of the Taylor series expansion. To demonstrate this important result, I combine equations (13a) (for α) and (13b) to give

$$\frac{\tau_q^2}{2\alpha} = \frac{\tau_q}{2}\left(\frac{\tau_q}{\alpha}\right) = \frac{1}{2}\frac{\tau_F^2(C_e+C_l)}{K}+\left(\frac{C_eC_l}{KG}\right)\tau_F + \frac{(C_eC_l)^2}{2KG^2(C_e+C_l)}. \tag{13d}$$

The first term on the right-hand side of (13d) is negligibly small because it is of the order of τ_F^2, refer to the consistent treatment in equation (1c). The third term on the right-hand side of equation (13d), on the other hand, can be arranged into the following form:

$$\frac{(C_eC_l)^2}{2KG^2(C_e+C_l)} = \frac{C_e^2}{2K(C_e+C_l)}\tau_T^2. \tag{13e}$$

It is proportional to τ_T^2 which is again negligibly small in consistency with the Taylor series expansion used in equation (11). The remaining expression of equation (13d) is thus identical to equation (13c). Using equation (13b) and the α-expression in (13a) gives the expression for the phase lag of the heat flux vector in terms of the *microscopic* properties:

Table 1. Correspondence of the dual-phase-lag model to diffusion, thermal wave, heat-flux equation of Jeffreys-type, phonon–electron interactions (parabolic and hyperbolic) and phonon scattering field theory in terms of τ_q and τ_T. $\tau_R \equiv$ the relaxation time in the Umklapp process; $\tau_N \equiv$ the relaxation time in the normal process; $\tau \equiv$ effective relaxation time in the Jeffreys model

Dual-phase-lag model	Diffusion	Classical CV-wave	Heat-flux equation of Jeffreys type	Phonon–electron interactions (parabolic)	Phonon–electron interactions (hyperbolic)	Phonon scattering field
τ_q	0	$\frac{\alpha}{C^2}$	τ	$\frac{1}{G}\left(\frac{1}{C_e}+\frac{1}{C_l}\right)^{-1}$	$\tau_F+\frac{1}{G}\left(\frac{1}{C_e}+\frac{1}{C_l}\right)^{-1}$	τ_R
τ_T	0	0	$k\tau$†	$\frac{C_l}{G}$	$\frac{C_l}{G}$	$\frac{9}{5}\tau_N$
α	α	α	α	$\frac{K}{C_e+C_l}$	$\frac{K}{C_e+C_l}$	$\frac{c^2\tau_R}{3}$

† The parameter k corresponds to the ratio of τ_T/τ_q, the parameter R in equation (18), in the dual-phase-lag model. In terms of the microscopic properties, $R = 1+(C_l/C_e)$ in correlation to the parabolic phonon–electron interaction model and $R = (9/5)(\tau_N/\tau_R)$ in correlation to the phonon scattering field.

Table 2. Equivalent thermal diffusivity (α_E), phase lags (τ_q and τ_T) and thermal wave speed (C_E). $C_e = 2.1\times10^4$ J m^{-3} K^{-1} at room temperature

	K (W m^{-1}K^{-1})	C_l (J m^{-3} K^{-1}) ($\times10^6$)	G (W m^{-3} K^{-1}) ($\times10^{16}$)	α_E (m^2 s^{-1}) ($\times10^{-4}$)	τ_F (ps)	τ_T (ps)	τ_q (ps)	C_E (m s^{-1}) $\times10^5$	$\sqrt{\alpha\tau_q}$ (ns)
Cu	386	3.4	4.8	1.1283	0.03	70.833	0.4648	2.7201	7.2418
Ag	419	2.5	2.8	1.6620	0.04	89.286	0.7838	2.1979	11.4135
Au	315	2.5	2.8	1.2495	0.04	89.286	0.7838	1.9058	9.8963
Pb	35	1.5	12.4	0.2301	0.005	12.097	0.1720	1.3718	1.9894

$$\tau_q = \tau_F + \frac{1}{G}\left(\frac{1}{C_e}+\frac{1}{C_l}\right)^{-1}. \tag{14}$$

In the previous work [34], perfect correlations were established between the dual-phase-lag model and (i) the parabolic two-step model assuming a diffusion behavior in the electron gas and (ii) the pure phonon scattering field theory describing the momentum loss of phonon collisions in the Umklapp process. In the presence of a *ballistic behavior* in the electron transport, again, a precise correlation exists, equation (13a) for α and τ_T and equation (14) for τ_q Table 1 summarize the correlations established so far, including the macroscopic diffusion and thermal wave models, the heat-flux equation of Jeffreys type [23], the microscopic parabolic and hyperbolic two-step models and the pure phonon scattering model. Indeed, the dual-phase-lag model covers a wide scale of physical responses in both space and time. Based on the experimental data for the heat capacities and the electron–phonon coupling factors [6–9, 32, 33], I further calculate the values of τ_T and τ_q according to equations (13a) and (14) for copper (Cu), silver (Ag), gold (Au) and lead (Pb). The results are given in Table 2. The value of τ_F is taken from the work by Qiu and Tien [11], which affects the heat transport process in two ways. It changes the value of τ_q (refer to equation (14)) and it brings in the third-order time-derivative in equation (8). While the former effect alters the value of τ_q by no more than 6%, the latter effect *completely* alters the way in which heat propagates through the medium. For the four representative metals shown in Table 2, the value of τ_T is approximately two orders of magnitude *larger* than that of τ_q. The apparent heat source in equation (12) (the dual-phase-lag model) contains an additional term, $\partial^2 S/\partial t^2$, in comparison with that in equation (8) (the hyperbolic two-step model). This term, however, is led by τ_q^2, which is of the order of 10^{-24} seconds. Contribution from this additional term seems to be negligibly small for the laser heating technology developed so far.

THE WAVE BEHAVIOR

Equation (12) introduces a strong *wave* behavior in heat propagation. This behavior is demonstrated by isolating the two *third-order* derivatives governing the fundamental characteristics of the solution:

$$\frac{\partial}{\partial t}\left(\frac{\partial^2 T}{\partial x^2}-\frac{1}{C^2}\frac{\partial^2 T}{\partial t^2}\right)+\text{lower order terms} = 0,$$

$$\text{with}\quad C = \sqrt{\frac{2\alpha\tau_T}{\tau_q^2}}. \tag{15}$$

Clearly, the temperature described by equation (15) propagates as a *wave* at a finite speed of C. In terms of the microscopic properties in the two-step model, according to equations (13a) and (14),

$$C = \sqrt{\frac{2\alpha\tau_T}{\tau_q^2}} = \sqrt{\frac{K}{\tau_F C_e}}. \quad (16)$$

The value of C approaches infinity as the relaxation time of electrons evaluated at the Fermi surface, τ_F, approaches zero. The thermal wave speed represented by equation (16) is attributed to the ballistic behavior of heat transport in the electron gas. It results from a *new-type* of wave equation, equation (12) describing the *microscale* effect in both *space* and *time*, and should not be confused with that in the *macroscopic* framework established by Cattaneo and Vernotte [26–28].

THE ONE-DIMENSIONAL WAVES

Equation (12) displays a new type of differential equation in conductive heat transfer. Reflected by the two delay times, τ_T and τ_q, in the *macroscopic* response between the heat flux and the temperature gradient, it combines the effect of microstructural interactions in the fast-transient process. I shall explore the wave structure behind equation (12) by considering temperature waves propagating in a semi-infinite medium. While the front surface is subjected to a sudden increase of temperature, the boundary extending to infinity facilitates a thorough examination of the way in which temperature decays and the heat affected zone evolves. Although the effect of apparent heating is interesting, it will be excluded it from this study because it does not contribute to the fundamental characteristics of the temperature waves.

For a more systematic study, the following dimensionless parameters are introduced:

$$\theta = \frac{T - T_0}{T_w - T_0}, \quad \beta = \frac{t}{\tau_q}, \quad \delta = \frac{x}{\sqrt{\alpha\tau_q}} \quad (17)$$

with T_w and T_0, respectively, being the suddenly raised temperature at the front surface at $x = 0$ and the initial temperature of the medium as $t = 0$. In terms of these variables, equation (12) becomes

$$\frac{\partial^2\theta}{\partial\delta^2} + R\frac{\partial^3\theta}{\partial\delta^2\,\partial\beta} = \frac{\partial\theta}{\partial\beta} + \frac{\partial^2\theta}{\partial\beta^2} + \frac{1}{2}\frac{\partial^3\theta}{\partial\beta^3}, \quad \text{with } R = \frac{\tau_T}{\tau_q}. \quad (18)$$

The boundary conditions are

$$\theta = 1 \quad \text{at} \quad \delta = 0, \quad \theta \to 0 \quad \text{as} \quad \delta \to \infty. \quad (19)$$

I need three initial conditions to formulate the effect of the third-order time-derivative in equation (18):

$$\theta = 0, \quad \frac{\partial\theta}{\partial\beta} = 0, \quad \frac{\partial^2\theta}{\partial\beta^2} = 0 \quad \text{as} \quad \beta = 0. \quad (20)$$

Although the effect of time-rate of changes is a special feature in this type of problem [34, 36, 37], I assume zero values for $\partial\theta/\partial\beta$ and $\partial^2\theta/\partial\beta^2$ in order not to disturb the wave structure.

The Laplace transform solution satisfying equations (18) to (20) can be easily obtained:

$$\theta = \frac{\exp\left(-\sqrt{\frac{p(2+2p+p^2)}{2(1+Rp)}}\,\delta\right)}{p}. \quad (21)$$

The Laplace inversion of equation (21), however, involves four branch points at $p = 0$, $-1/R$, $(1+i)$ and $(1-i)$ in the Bromwich contour integral. The final result can be simplified to an improper integral but a numerical evaluation is still unavoidable. Therefore, I apply the numerical inversion formula developed previously [34, 36] to invert equation (21):

$$\theta(\delta,\beta) = \frac{e^{\gamma\beta}}{\beta}\left(\frac{\bar\theta(\delta,\gamma)}{2} + Re\sum_{n=1}^{N}(-1)^n\bar\theta\left(\delta,\gamma+\frac{in\pi}{\beta}\right)\right). \quad (22)$$

Equation (22) is actually the Riemann sum approximation of the *Fourier* integral transformed from the Laplace inversion integral. The quantity γ is the real value in the Bromwich cut from $\gamma - i\infty$ to $\gamma + i\infty$. For a faster convergence, the value of γ satisfies the relation

$$\gamma\beta \simeq 4.7 \quad (23)$$

with β being the dimensionless physical time. At $\beta = 1$, for example, a value of 4.7 should be used for γ. Other values of γ will lead to the same solution, but the number of terms needed in the summation of equation (22), especially for problems involving discontinuities at the sharp wavefront, will increase by orders of magnitude for convergence [34, 36, 37]. In this work, the summation in equation (22) is performed until the Cauchy norm is smaller than or equal to 10^{-15}.

For easier identification with various other models, artificially include two coefficients A and B into equation (18):

$$\frac{\partial^2\theta}{\partial\delta^2} + R\frac{\partial^3\theta}{\partial\delta^2\,\partial\beta} = \frac{\partial\theta}{\partial\beta} + A\frac{\partial^2\theta}{\partial\beta^2} + B\frac{\partial^3\theta}{\partial\beta^3}. \quad (24)$$

The case of $A = 1$ and $B = \frac{1}{2}$ is equivalent to the hyperbolic two-step model, equation (18). The case of $A = 1$ and $B = 0$ reduces to the parabolic two-step model where only the *linear* terms in τ_T and τ_q are retained in equation (11). The case of $A = 1$, $B = 0$ and $R = 0$ reduces to the classical thermal wave model employing the *single*-phase-lag concept ($\tau_T = 0$). Finally, the case of $A = 1$, $B = 0$ and $R = 1$ ($\tau_T = \tau_q$) reduces to the classical diffusion model without the lagging response [38]. Equation (24), based on the dual-phase-lag concept, thus covering a wide scale of space and time for physical observations.

Figure 1 shows the temperature distributions for $R = 100$ and $\beta = 1$. The dual-phase-lag model with the τ_q^2-effect ($A = 1$ and $B = \frac{1}{2}$, the hyperbolic two-step model) predicts a sharp wavefront at

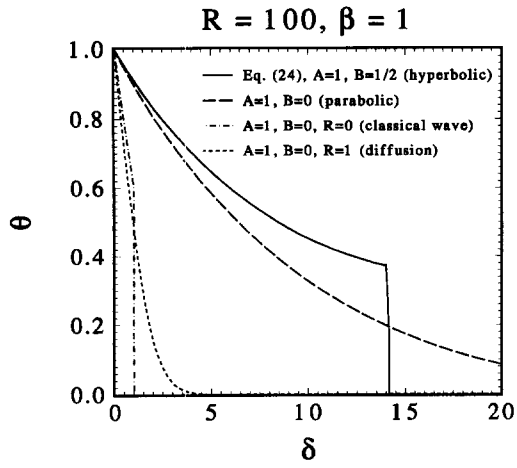

Fig. 1. Temperature distribution predicted by the dual-phase-lag model. Equation (24) with $A = 1$ and $B = \frac{1}{2}$ (corresponding to the hyperbolic two-step model), $A = 1$ and $B = 0$ (the parabolic two-step model), $A = 1$, $B = 0$ and $R = 0$ (the classical thermal wave model) and $A = 1$, $B = 0$ and $R = 1$ (the diffusion model).

$\delta = \sqrt{2R\beta} \simeq 14.14214$. This is the most distinguishable effect from the ballistic behavior of heat transport in electrons (the τ_q^2-effect), even more so than the value of τ_q being slightly modified by the relaxation time τ_F. The classical thermal wave model to diffusion, in large, is what the hyperbolic two-step model is to the parabolic two-step model. The effect of microstructural interactions absorbed in the phase lag of the temperature gradient, τ_T, however, induces a *much larger* heat-affected zone and *much higher* temperature level in the heat-affected zone. They are major reasons leading to the successful prediction of the sub-picosecond surface reflectivity in gold films [10]. Figure 2 displays the effect of the ratio of τ_T to τ_q on the propagation of temperature waves. The location of the thermal wavefront, to be reiterated, is at $\delta = \sqrt{2R\beta}$ under various values of R. At the same instant of time, the thermal penetration depth into the solid increases with the ratio of R in a square-root sense. This is also the effect of microstructural interactions because the ratio R is proportional to τ_T. The effect of fast-transients is absorbed in τ_q. It provides a counter-balanced effect with regard to the thermal penetration depth. Figure 3 displays the time-history of temperature waves at $\beta = 1, 2, 3$ and 4 (the instant of time beyond which the sharp thermal wavefront vanishes). For responses at longer times, evidenced by the distributions of $R = 10$ as $\beta = 3$ and 4, the temperature levels off when approaching the sharp wavefront. It then drops to zero in the thermal undisturbed zone. This is a unique behavior pertinent to the effect of τ_q^2 (the ballistic behavior in electron transport from a microscopic point of view) and is not found in the macroscopic thermal wave theory.

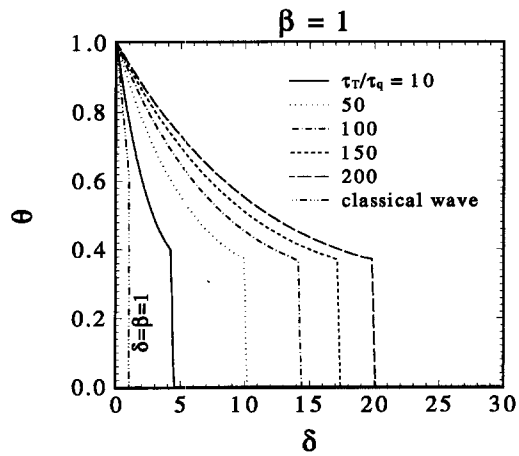

Fig. 2. Evolution of temperature waves described by equation (18) with the ratio of $R = \tau_T/\tau_q$. The thermal wave front is located at $\delta = \sqrt{2R\beta}$.

From a consistent mathematical point of view, the second-order expansions in τ_T and τ_q should also involve a second-order time-derivative in τ_T^2 on the right-hand side of equation (11):

$$q(x,t) + \tau_q \frac{\partial q}{\partial t}(x,t) + \frac{\tau_q^2}{2}\frac{\partial^2 q}{\partial t^2}(x,t) \simeq -K\left(\frac{\partial T(x,t)}{\partial x} + \tau_T \frac{\partial^2 T(x,t)}{\partial x\,\partial t} + \frac{\tau_T^2}{2}\frac{\partial^3 T(x,t)}{\partial x\,\partial t^2}\right). \quad (25)$$

The new τ_T^2-effect induces an additional fourth-order derivative in equation (12), resulting in an equation of *parabolic type* again. In absence of the heating terms, equation (12) becomes

$$\frac{\partial^2 T}{\partial x^2} + \tau_T \frac{\partial^3 T}{\partial x^2\,\partial t} + \frac{\tau_T^2}{2}\frac{\partial^4 T}{\partial x^2\,\partial t^2} = \frac{1}{\alpha}\frac{\partial T}{\partial t} + \frac{\tau_q}{\alpha}\frac{\partial^2 T}{\partial t^2} + \frac{\tau_q^2}{2\alpha}\frac{\partial^3 T}{\partial t^3}. \quad (26)$$

Its dimensionless form corresponding to equation (18) is

$$\frac{\partial^2 \theta}{\partial \delta^2} + R\frac{\partial^3 \theta}{\partial \delta^2\,\partial \beta} + \frac{R^2}{2}\frac{\partial^4 \theta}{\partial \delta^2\,\partial \beta^2} = \frac{\partial \theta}{\partial \beta} + \frac{\partial^2 \theta}{\partial \beta^2} + \frac{1}{2}\frac{\partial^3 \theta}{\partial \beta^3}, \quad \text{with} \quad R = \frac{\tau_T}{\tau_q}. \quad (27)$$

The fourth-order derivative characterizes the fundamental structure of equation (27). It gives a parabolic nature to equation (27) and diminishes the wave behavior argued in equation (15). Under the same initial and boundary conditions given in equation (19) and (20), Fig. 4 displays the solutions of equation (18) (the effect of τ_q^2 alone) and equation (27) (both effects of τ_T^2 and τ_q^2). Exemplified by the case of $\beta = 1$ and $R = 150$, the effect of τ_T^2 not only diminishes the sharp wavefront, but also extends the heat-affected zone *deeper* into the medium.

In passing, note that the observation time and physical space have been normalized with respect to the relation time τ_q and the equivalent length-scale $l = \sqrt{\alpha\tau_q}$. For metals, these variables imply the real

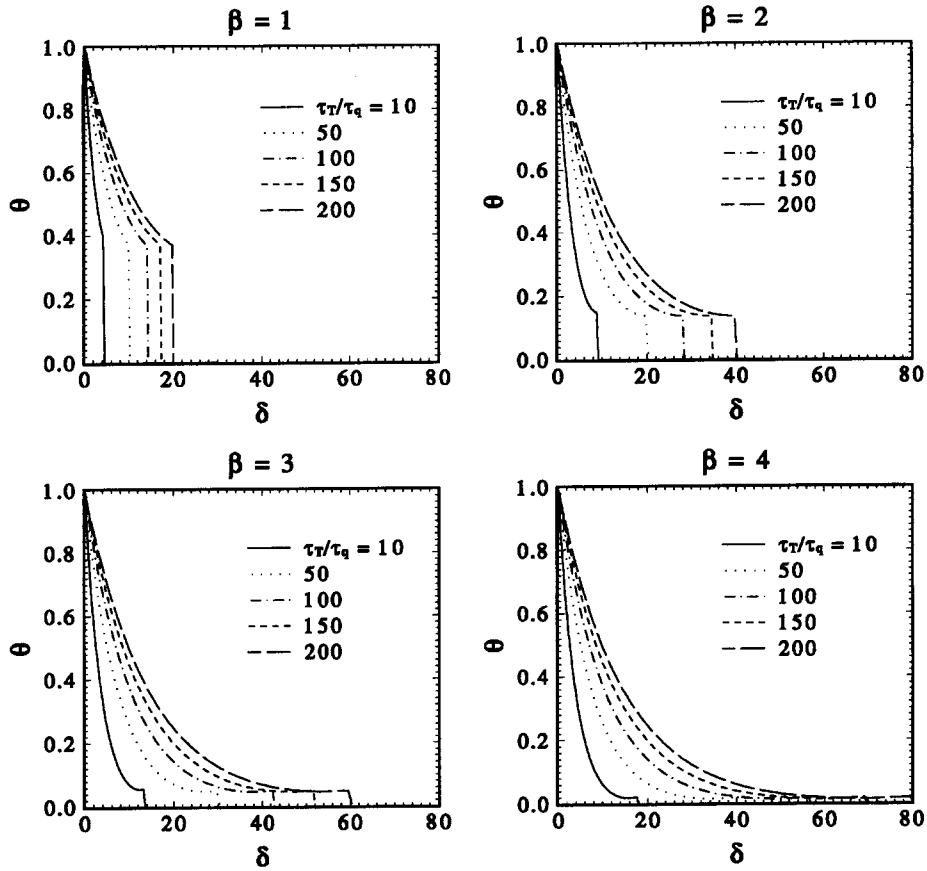

Fig. 3. Time-history of the temperature waves described by equation (18) at various values of R. $\beta = 1$, 2, 3 and 4.

scales of picoseconds in time and nanometers in space for the response curves shown in Figs. 1–4.

CONCLUSION

A macroscopic dual-phase-lag model is proposed in this work to incorporate the effect of microstructural interactions in the fast-transient process of heat transport. The unique feature lies in viewing the presence of microstructural interactions as *retarding sources* causing a macroscopic *delayed* response in time. Preliminary success of this approach is measured by its precise correlation with the existing microscopic (both the hyperbolic and parabolic two-step and the pure phonon scattering) and macroscopic (diffusion and wave) models. The generalized lagging response described in the framework of the two phase lags evidently covers a wide scale of space and time for physical observations. As a result, there is no need to switch from one model (such as diffusion or wave) to another (such as phonon–electron interaction or pure phonon scattering) associated with shortening of the response time. Because of the absence of a quantitative criterion depicting the applicable regimes of these models, the model-switching not only heavily relies on experience but also risks the loss of important information describing the way(s) in which a certain macroscopic behavior transits into a microscopic response in the time-frame. The proposed dual-phase-lag concept seems able to remove this ambiguity. Most importantly, it adopts a macroscopic approach already familiar to practicing engineers. It thus facilitates a smoother transition in describing heat transport from a macroscopic to a microscopic level.

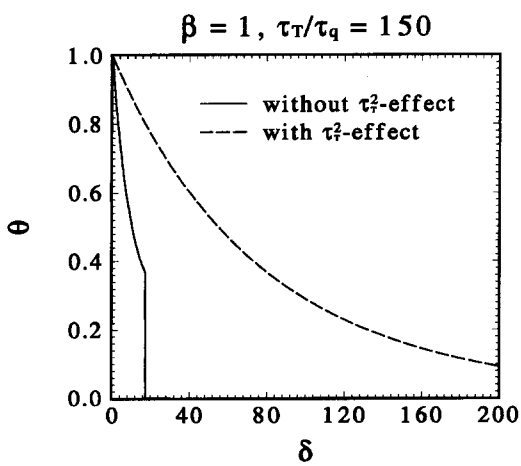

Fig. 4. Diminution of the sharp wavefront by the τ_T^2-effect. Comparison of equations (18) and (27).

Within the framework of the dual-phase-lag model,

the effect of microstructural interactions is largely absorbed in the phase lag of the *temperature gradient* (τ_T) while the effect of fast-transients is absorbed in the phase lag of the *heat flux vector* (τ_q). The effect of τ_q is mainly responsible for the presence of a sharp wavefront in heat propagation, as reflected by the cases of $\tau_T = 0$ (the classical thermal waves) and the τ_q^2-effect in equation (18) (the ballistic behavior of heat transport in electrons). The effect of τ_T, on the other hand, diminishes the sharp wavefront and extends the heat-affected zone *deeper* into the solid medium. When the microstructural effect (the τ_T-effect) is present in heat transport, the distribution curve of temperatures displays a monotonically decaying behavior similar to diffusion. The temperature level and the physical dimension of the heat-affected zone, however, are much larger than those predicted by the diffusion model assuming an instantaneous response and a quasi-equilibrium transition between thermodynamic states. Because the effect of τ_T induces higher order derivatives in time, in addition, equation (14) allows specifications of the time-rate of changes of temperature, $\partial T/\partial t$ and $\partial^2 T/\partial t^2$ in the initial conditions. As shown by Tzou [34] for the correlation with the parabolic two-step model, such a *rate-effect* will intrinsically alter the temperature distributions.

The perfect correlations made with the microscopic models shown in Table 1 determine the precise values of the two phase lags in the range of pico- to femtoseconds. For transient processes occurring in submicroseconds, such as those in reticulated metallic structures or some composites with insulator-like materials as the second phase constituents, the two phase lags have to be determined by the transient-time experiments incorporated with the microscopic support for the governing mechanisms.

The transient experiment on the medium blasting sand has had to be performed with the cooperation of colleagues and details are given in ref. [38]. The particle size in this medium ranges from dust to 2 mm, having a mean value of 0.2 mm. The *delayed response* in this case is due to the *finite time* required for the heat flow to circulate around pores. Comparing with the experimental result, the classical wave model may *overestimate* the peak value of transient temperatures by as much as 100%, depending on the pulse-width and the location from the heater. The dual-phase-lag model, on the other hand, accurately describes the entire transient response. The two phase lags, τ_q and τ_T respectively, have been found to be 4.48 s and 8.94 s at a distance of 0.4 mm (twice the mean-particle-size) from the heater. These values, however, degrade non-homogeneously in a direction away from the heater because of the *gradient* of the discrete structures.

REFERENCES

1. I. W. Boyd, *Laser Processing of Thin Films and Microstructures*. Springer, New York (1989).
2. J. A. Knapp, P. Børgesen and R. A. Zuhr, *Beam-Solid Interactions: Physical Phenomena. (Materials Research Society Symposiums and Proceedings)*, Vol. 157. Materials Research Society, Pittsburgh, PA (1990).
3. G. Chryssolouris, *Laser Machining, Theory and Practice*. Springer, New York (1991).
4. D. E. Koshland, Special section: Engineering a small world, from atomic manipulation to microfabrication, *Science* **254,** 1300–1342 (1991).
5. J. Narayan, V. P. Godbole and G. W. White, Laser method for synthesis and processing of continuous diamond films on nondiamond substrates, *Science* **52,** 416–418 (1991).
6. J. G. Fujimoto, J. M. Liu and E, P. Ippen, Femtosecond laser interaction with metallic tungsten and non-equilibrium electron and lattice temperature, *Phys. Rev.* **53,** 1837–1840 (1984).
7. S. D. Brorson, J. G. Fujimoto and E. P. Ippen, Femtosecond electron heat-transport dynamics in thin gold film, *Phys. Rev. Lett.* **59,** 1962–1965 (1987).
8. S. D. Brorson, A. Kazeroonian, J. S. Moodera, D. W. Face, T. K. Cheng, E. P. Ippen, M. S. Dresselhaus and G. Dresselhaus G., Femtosecond room-temperature measurement of the electron–phonon coupling constant λ in metallic superconductors, *Phys. Rev. Lett.* **64,** 2172–2175 (1990).
9. H. E. Elsayed-Ali, Femtosecond thermoreflectivity and thermotransmissivity of polycrystalline and single-crystalline gold films, *Phys. Rev.* **B43,** 4488–4491 (1991).
10. T. Q. Qiu and C. L. Tien, Short-Pulse Laser Heating on Metals, *Int. J. Heat Mass Transfer* **35,** 719–726 (1992).
11. T. Q. Qiu and C. L. Tien, Heat transfer mechanisms during short-pulse laser heating of metals, *ASME J. Heat Transfer* **115,** 835–841 (1993).
12. R. A. Guyer and J. A. Krumhansl, Solution of the linearized Boltzmann equation, *Phys. Rev.* **148,** 766–778 (1966).
13. Y. Bayazitoglu and G. P. Peterson (Eds), *Fundamental Issues in Small Scale Heat Transfer*, 1992 *ASME Winter Annual Meeting*, ASME HTD-Vol. 227 (1992).
14. F. M. Garner and K. S. Udell (Eds), *Heat Transfer on Microscale*, 1993 *National Heat Transfer Conference*, ASME HTD-Vol. 253 (1993).
15. C. L. Tien and G. Chen, Challenges in microscale conductive and radiative heat transfer, *ASME J. Heat Transfer* **116,** 799–807 (1994).
16. D. Y. Tzou, On the thermal shock wave induced by a moving heat source, *ASME J. Heat Transfer* **111,** 232–238 (1989).
17. D. Y. Tzou, Shock wave formation around a moving heat source in a solid with finite speed of heat propagation, *Int. J. Heat Mass Transfer* **32,** 1979–1987 (1989).
18. D. Y. Tzou, Thermal shock waves induced by a moving crack, *ASME J. Heat Transfer* **112,** 21–27 (1990).
19. D. Y. Tzou, Thermal shock waves induced by a moving crack—a heat flux formulation, *Int. J. Heat Mass Transfer* **33,** 877–885 (1990).
20. D. Y. Tzou, Thermal resonance under frequency excitations, *ASME J. Heat Transfer* **114,** 310–316 (1992).
21. D. Y. Tzou, Damping and resonance characteristics of thermal waves, *ASME J. Appl. Mech.* **59,** 862–867 (1992).
22. D. Y. Tzou, Thermal shock phenomena under high-rate response in solids. In *Annual Review of Heat Transfer* (Edited by Chang-Lin Tien), Chap. 3, pp. 111–185. Hemisphere, Washington, DC (1992).
23. D. D. Joseph and L. Preziosi, Heat waves, *Rev. Mod. Phys.* **61,** 41–73 (1989).
24. D. D. Joseph and L. Preziosi, Addendum to the paper on heat waves, *Rev. Mod. Phys.* **62,** 375–391 (1990).
25. M. N. Özisik and D. Y. Tzou, On the wave theory in heat conduction, *ASME J. Heat Transfer* **116,** 526–535 (1994).
26. C. Cattaneo, A form of heat conduction equation which

eliminates the paradox of instantaneous propagation, *Compte Rendus* **247,** 431–433 (1958).
27. P. Vernotte, Les paradoxes de la théorie continue de l'équation de la chaleur, *Compte Rendus* **246,** 3154–3155 (1958).
28. P. Vernotte, Some possible complications in the phenomena of thermal conduction, *Compte Rendus* **252,** 2190–2191 (1961).
29. D. Y. Tzou, An engineering assessment of the relaxation time in the thermal wave theory, *Int. J. Heat Mass Transfer* **36,** 1845–1851 (1993).
30. M. I. Kaganov, I. M. Lifshitz and L. V. Tanatarov, Relaxation between electrons and crystalline lattices, *Sov. Phys.–JETP* **4,** 173–178 (1957).
31. S. I. Anisimov, B. L. Kapeliovich and T. L. Perel'man, Electron emission from metal surfaces exposed to ultrashort laser pulses, *Sov. Phys.–JETP* **39,** 375–377 (1974).
32. H. E. Elsayed-Ali, T. B. Norris, M. A. Pessot and G. A. Mourou, Time-resolved observation of electron–phonon relaxation in copper, *Phys. Rev. Lett.* **58,** 1212–1215 (1987).
33. R. H. M. Groeneveld, R. Sprik, M. Wittebrood and A. Lagendijk, Ultrafast relaxation of electrons probed by surface plasmons at a thin silver film. In *Ultrafast Phenomena VII* (Edited by C. B. Harris *et al.*), pp. 368–370 Springer, Berlin (1990).
34. D. Y. Tzou, A unified field approach for heat conduction from macro- to micro-scales, *ASME J. Heat Transfer* **117,** 8–16 (1995).
35. J. I. Frankel, B. Vick and M. N. Özisik, Flux formulation of hyperbolic heat conduction, *J. Appl. Phys.* **58,** 3340–3345 (1985).
36. D. Y. Tzou, M. N. Özisik and R. J. Chiffelle, The lattice temperature in the microscopic two-step model, *ASME J. Heat Transfer* **116,** 1034–1038 (1994).
37. R. J. Chiffelle, On the wave behavior and rate effect of thermal and thermomechanical waves, M. S. Thesis, The University of New Mexico, Albuquerque, NM (1994).
38. D. Y. Tzou, Y. Zhang, J. R. Leith, Y. S. Xu, Y. K. Guo and Z. Y. Guo, The nonhomogeneous lagging response in porous media, *Int. J. Heat Mass Transfer* (submitted).